Neuron, Vol. 40, 775–784, November 13, 2003, Copyright ©2003 by Cell Press

The NMDA Receptor Is Coupled to the ERK Pathway by a Direct Interaction between NR2B and RasGRF1

Grigory Krapivinsky,[1] Luba Krapivinsky,[1] Yunona Manasian,[1] Anton Ivanov,[2] Roman Tyzio,[2] Christophe Pellegrino,[2] Yehezkel Ben-Ari,[2] David E. Clapham,[1,*] and Igor Medina[2]

[1]Howard Hughes Medical Institute
Children's Hospital
1309 Enders Building
320 Longwood Avenue
Boston, Massachusetts 02115

[2]INMED/INSERM Unite 29
163 Route de Luminy
13009 Marseille
France

Summary

The NMDA subtype of glutamate receptors (NMDAR) at excitatory neuronal synapses plays a key role in synaptic plasticity. The extracellular signal-regulated kinase (ERK1,2 or ERK) pathway is an essential component of NMDAR signal transduction controlling the neuroplasticity underlying memory processes, neuronal development, and refinement of synaptic connections. Here we show that NR2B, but not NR2A or NR1 subunits of the NMDAR, interacts in vivo and in vitro with RasGRF1, a Ca^{2+}/calmodulin-dependent Ras-guanine-nucleotide-releasing factor. Specific disruption of this interaction in living neurons abrogates NMDAR-dependent ERK activation. Thus, RasGRF1 serves as NMDAR-dependent regulator of the ERK kinase pathway. The specific association of RasGRF1 with the NR2B subunit and study of ERK activation in neurons with varied content of NR2B suggests that NR2B-containing channels are the dominant activators of the NMDA-dependent ERK pathway.

Introduction

Agonist binding of the NMDA receptor (NMDAR) increases postsynaptic $[Ca^{2+}]_i$ (Ghosh and Greenberg, 1995) and activates multiple signaling cascades, including the ERK pathway (Sweatt, 2001). In neurons, the ERK signaling cascade is a key step in regulatory pathways of cell survival (Grewal et al., 1999; Bonni et al., 1999) and neuronal plasticity, including different forms of LTP (Impey et al., 1999) and long-term memory (Adams and Sweatt, 2002). Downstream targets of ERK include transcription factors (Platenik et al., 2000; West et al., 2001; Abel and Lattal, 2001) required for synaptic plasticity and activity-dependent AMPA receptor trafficking to postsynaptic membranes (Zhu et al., 2002). ERK activity in neurons is regulated by many extracellular signals via multiple signaling pathways (Sweatt, 2001). NMDAR-dependent activation of ERK protein kinases requires Ca^{2+} entry (Bading and Greenberg, 1991; Kurino et al., 1995) and involves the small GTP binding protein Ras (Iida et al., 2001). The NMDAR-initiated ERK activation is sensitive to Ca^{2+} elevation spatially restricted to the vicinity of the NMDAR (Hardingham et al., 2001), suggesting close colocalization between NMDA receptors and sensory molecules.

Two molecules, SynGAP and RasGRF1, are candidates for linking NMDA receptor activation and Ca^{2+} influx with Ras and downstream cascades including ERK. SynGAP is a RasGTPase-activating protein localized exclusively to postsynaptic densities (Chen et al., 1998; Kim et al., 1998). SynGAP phosphorylation by Ca^{2+}/calmodulin-dependent kinase II (CaMKII) decreases its activity (Chen et al., 1998), making SynGAP a potential Ca^{2+} sensor (but see Oh et al., 2002). RasGRF1 is a Ras-specific GDP/GTP exchange factor (GEF) and Ras activator (Shou et al., 1992). RasGRF1 is selectively expressed in the central nervous system (CNS) and is enriched in synapses (Sturani et al., 1997; Zippel et al., 1997). Unlike other known GEFs, RasGRF1 activates Ras only when it binds Ca^{2+}/calmodulin (Farnsworth et al., 1995) and is thus a potential target of Ca^{2+} entering neurons. The gene for RasGRF1 was disrupted in two separate mouse studies (Brambilla et al., 1997; Giese et al., 2001). One group showed that the mice had impaired amygdala-dependent learning and memory (Brambilla et al., 1997). Cultures of embryonic RasGRF1$^{-/-}$ hippocampal neurons showed increased spontaneous neuronal activity and hyperexcitability (Tonini et al., 2001). Another group (Giese et al., 2001) reported that RasGRF1$^{-/-}$ mice had impaired hippocampus-related memory.

Here we show that RasGRF1 specifically binds the NMDA receptor subunit, NR2B, in vitro and in vivo. Disruption of this interaction in living neurons impaired NMDAR-dependent ERK activation, suggesting a specific role for the NR2B subunit in coupling the NMDAR to ERK.

Results

NR2B Directly Interacts with RasGRF1

Yeast two-hybrid screening of a rat brain library with a bait containing a portion of the NR2B cytoplasmic C-terminal domain (amino acids 886–1310) yielded five independent clones encoding the C-terminal portion of RasGRF1 (accession # P28818). These results suggest that NR2B directly interacts with RasGRF1.

The interaction of NR2B and RasGRF1 was further tested with purified proteins. The interacting C-terminal fragment of NR2B (886–1310), affinity purified from bacteria as a NusA fusion protein, bound in vitro translated RasGRF1 (Figure 1A). Full-length RasGRF1 and NR2B co-expressed in HEK293T cells formed a complex that was co-immunoprecipitated by NR2B antibody (Figure 1B). Since native neuronal NMDA receptors at mature synapses are heteromers of NR1 and one or more subtypes of NR2 (Cull-Candy et al., 2001), we tested whether RasGRF1 also associated with NR2A or NR1. As shown

*Correspondence: dclapham@enders.tch.harvard.edu

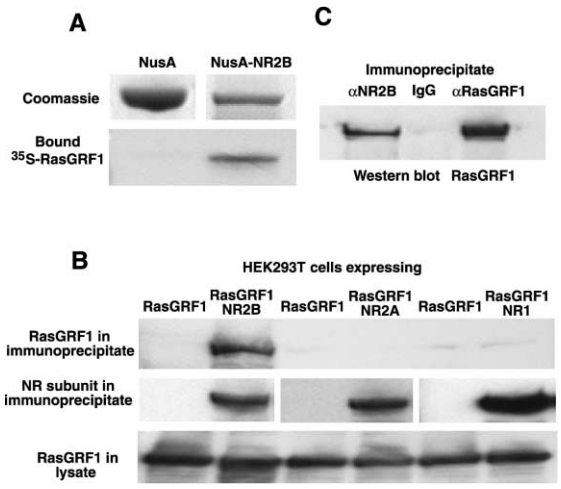

Figure 1. NR2B and RasGRF1 Interact In Vitro and In Vivo

(A) A purified 6His-NusA-NR2B(886–1310) fusion protein specifically precipitated in vitro translated RasGRF1.

(B) Interaction of RasGRF1 and NMDA subunits co-expressed in HEK293T cells.

(C) RasGRF1 and NR2B co-immunoprecipitated from rat brain microsomes.

in Figure 1B, RasGRF1 did not co-immunoprecipitate either NR1 or NR2A from HEK293T cells co-expressing these subunits. Finally, NR2B and RasGRF1 were co-immunoprecipitated from solubilized rat brain microsomes (Figure 1C) or from 14-day-old primary cultures of dissociated rat neonatal hippocampal neurons (not shown). These data provide evidence that NR2B and RasGRF1 interact directly and associate in a molecular complex in native neurons.

Minimal Interacting Fragments as Binding Domains

In order to determine the signal transduction pathway dependent on NR2B-RasGRF interaction, we developed tools to specifically disrupt this *interaction*. The advantage of this approach over disrupting the gene or overexpressing the protein is that the interaction can be specifically targeted in vivo, without disturbing other components of the system. Minimal interacting fragments on both NR2B and RasGRF1 molecules were identified, and the peptides encoding these interacting fragments were tested for their ability to interfere with NR2B-RasGRF1 interactions.

The domain of NR2B interacting with RasGRF1 (NR2B-BD) and the domain of RasGRF1 interacting with NR2B (RasGRF1-BD) were determined by binding in vitro translated full-length molecules with in vitro translated epitope-tagged fragments of NR2B or RasGRF1, respectively (Figures 2A and 2B). The N-terminal portion of RasGRF1, which contains multiple functional domains (amino acids 1–720; Figure 2A), did not bind NR2B. In contrast, the C-terminal prey-containing sequence bound NR2B (amino acids 714–1244; Figure 2B). The distal portion of the C terminus containing the catalytic domain (amino acids 914–1244) was not essential for binding NR2B, while the region between the second PH domain and the catalytic domain (amino acids 714–913) was sufficient for NR2B binding. This domain is present only in neuron-specific RasGRF1; it is absent in the otherwise homologous, ubiquitously expressed, RasGRF2. The shorter peptides (amino acids 714–841 and 835–913) did not bind NR2B (Figure 2B). Thus, truncation of the RasGRF1-specific sequence from either the C or N terminus resulted in loss of binding, suggesting that several separated protein segments may be responsible for specific interactions. Therefore, the RasGRF1 domain interacting with NR2B is localized between amino acids 714–913 of RasGRF1. The peptide encoding this region of RasGRF1 was designated as the RasGRF1-BD and used in subsequent experiments.

The NR2B bait (amino acids 886–1310) bound RasGRF1 in vivo and in vitro (Figure 1A). This entire amino acid segment of NR2B constituted the best interacting peptide; a peptide encoding the distal portion of the bait (amino acids 1136–1310) did not bind RasGRF1 in vitro, and a peptide with a shorter C-terminal segment (amino acids 886–1219) bound RasGRF1 in vitro less efficiently than the 886–1310 bait (Figure 2C). Therefore, the NR2B 886–1310 peptide was used as the NR2B-BD in subsequent competition studies.

To test whether NR2B-BD and RasGRF1-BD peptides were sufficient to disrupt the interaction between NR2B and RasGRF1 in the native complex, we immunoprecipitated NR2B-RasGRF1 complexes from 6- to 8-week-old rat brains in the presence of purified NR2B-BD and RasGRF1-BD NusA fusion proteins. Both NR2B- and RasGRF1-BD fusion proteins (3–5 μM) completely blocked co-immunoprecipitation of NR2B and RasGRF1 (Figure 2D). Thus, both NR2B- and RasGRF1-BD were sufficient to disrupt the NR2B/RasGRF1 native complex.

Disruption of NR2B-RasGRF1 Interaction Abrogates NMDAR-Dependent ERK Activation

Since RasGRF1 is a Ca^{2+}/calmodulin-dependent activator of Ras (Farnsworth et al., 1995) and Ca^{2+} entering the neuron through the NMDAR channel activates the ERK pathway (Xia et al., 1996), we hypothesized that NR2B bound RasGRF1 transduces the signal from the NMDAR to ERK. To test this hypothesis, a dominant-negative (DN) form of RasGRF1 (Vanoni et al., 1999) was expressed in cultured hippocampal neurons and its effect on ERK activation tested. The activity of ERK was evaluated by immunostaining with an antibody recognizing the active (phosphorylated) ERK (Payne et al., 1991). As shown in Figure 3B, RasGRF1-DN significantly suppressed NMDA- and bicuculline-induced ERK activation. Overexpression of RasGRF1-DN did not significantly affect BDNF- and depolarization-dependent ERK activation.

If NR2B-RasGRF1 interaction is critical for signal transduction from the NMDAR to ERK activation, then disruption of this interaction should prevent NMDA-dependent ERK activation. To disrupt the RasGRF1-NR2B interaction in living neurons, we transfected primary cultures of hippocampal neurons with enhanced green fluorescent protein (EGFP) fused to binding domains of NR2B or RasGRF1. The expression of fusion proteins encoding the entire binding domains resulted in a striking decrease in the level of NMDAR-dependent ERK activation compared to control nontransfected

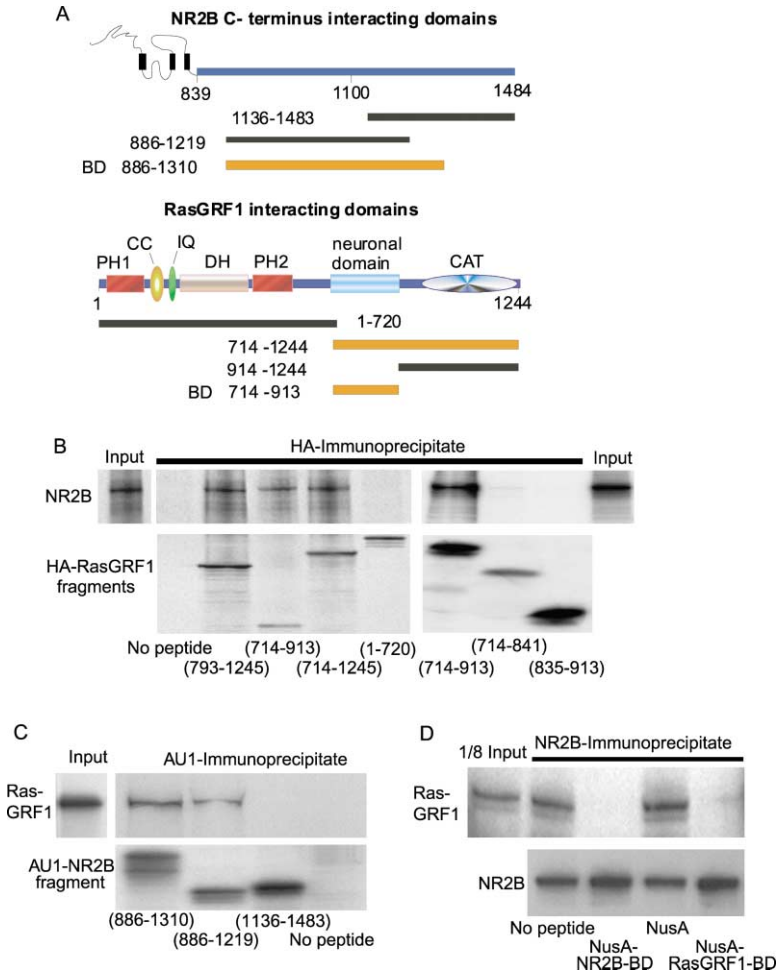

Figure 2. RasGRF1 and NR2B Binding Domains

(A) Map of the regions of NR2B and RasGRF1 DNAs used for the in vitro interaction assay. PH, plekstrin homology domain; CC, coiled coil domain; IQ, CaM binding domain; DH, DBL-homology domain.

(B) RasGRF1 fragments bound full-length NR2B in vitro. In vitro translated full-length NR2B and HA-tagged RasGRF1 fragments were co-immunoprecipitated with anti-HA antibody. The right lower panel is shifted up relative to the lower left panel.

(C) In vitro translated full-length RasGRF1 and AU1-tagged NR2B fragments were co-immunopecipitated with AU1 antibody.

(D) Blocking peptides (RasGRF1-BD and NR2B-BD) dissociate RasGRF1 and NR2B in native complexes isolated from rat brain. NR2B was immunoprecipitated from brain microsome lysates in the presence of purified NusA-RasGRF1-BD or NusA-NR2B-BD, and the immunoprecipitate was probed with anti-RasGRF1 antibody.

neurons or neurons expressing GFP alone (Figures 3A and 3B). Expressed binding domains are large peptides and thus may contain regions interacting with other molecules, but smaller fragments were ineffective in binding assays (Figures 2B and 2C). The BD fragments that were ineffective in binding nonetheless contained large binding domain segments and were used as additional controls to rule out the possibility of a nonspecific ERK activation (Figure 3C). Thus, expression of the dominant-negative form of RasGRF1, the complete BDs (but not overlapping peptides encoding only portions of the binding domains), effectively inhibited the NMDAR-dependent activation of ERK. These data support the hypothesis that a direct link between NR2B and RasGRF1 is critical for NMDAR-specific ERK activation.

Neuronal ERK activity is regulated by several signals, including Ca^{2+} influx through the L-type voltage-dependent Ca^{2+} channel (Dolmetsch et al., 2001) and BDNF-mediated pathways (Bonni et al., 1999). To determine whether expression of NR2B-BD or RasGRF1-BDs specifically interrupted NMDAR-mediated ERK activation rather than simply inhibiting ERK activity, NMDA-independent stimuli were used to activate ERK. As shown in Figure 3B, the expressed NR2B- and RasGRF1-BD peptides had no effect on depolarization- or BDNF-induced ERK activation. Furthermore, NMDAR-dependent phosphorylation of the CREB transcription factor (Ginty et al., 1993; Xia et al., 1996) was not affected by NR2B- or RasGRF1-BD expression (data not shown), indicating that the NMDAR pathway upstream of RasGRF1 was not affected.

The RasGRF1 locus interacting with NR2B also interacts with CaMKII (Bayer et al., 2001). Might the NR2B-BD peptide also block NMDAR-dependent ERK activity by inhibiting CaMKII activation? To test this possibility, we examined whether inhibition of CaMKII activity affected NMDAR-dependent ERK activation. Application of KN-93 (a cell-permeable, CaMKII-selective inhibitor) altered neither NMDA- nor bicuculline-dependent ERK activation, nor did it affect NR2B-BD or RasGRF1-BD peptide block of ERK activation (Figure 3C). In control experiments, KN93 effectively suppressed the phosphorylation of CREB and SynGAP in cultured hippocampal neurons (not shown). Thus, under these conditions, NMDAR-dependent ERK activation did not require CaMKII activity. We conclude that if NR2B-BD interfered with NR2B-CaMKII interactions, it did not significantly affect NMDAR-dependent ERK activation.

Expression of RasGRF1-BD or NR2B-BD could conceivably affect ERK activation upstream of RasGRF1 by decreasing NMDAR currents, and thus local $[Ca^{2+}]_i$. To test this possibility, we studied the properties of the NMDAR-mediated currents in neurons expressing BD fusion constructs. The expression of either binding do-

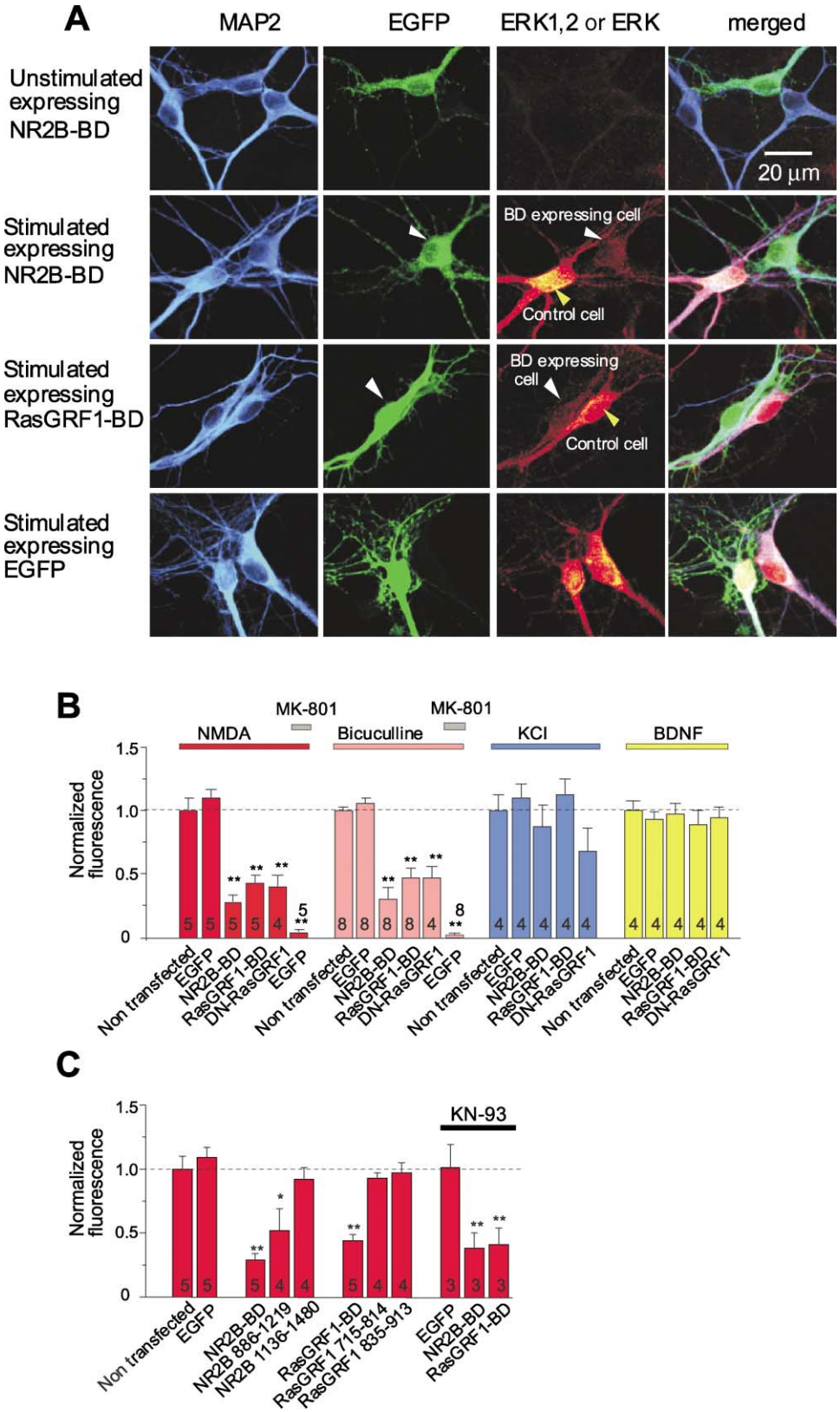

Figure 3. Blocking Peptides RasGRF1-BD and NR2B-BD Expressed in Cultured Hippocampal Neurons Inhibit NMDAR-Dependent Activation of ERK1,2

(A) Images of activated (phosphorylated) ERK in neurons expressing EGFP, EGFP-NR2B-BD, or EGFP-RasGRF1-BD.

(B) Population data summarizing the effect of NR2B-BD, RasGRF1-BD, and DN-RasGRF1 on NMDA, bicuculline, KCl, or BDNF-induced ERK phosphorylation. 10 μM MK-801 was applied to confirm the NMDAR dependence of ERK activation.

(C) Nonbinding fragments of NR2B-BD, RasGRF1-BD did not affect NMDA-dependent ERK activation. 5 μM KN-93 in the incubation media also had no effect on NMDA-dependent ERK activation. Bars show average phospho-ERK fluorescence normalized to the fluorescence of EGFP-transfected cells ± SEM; numbers of independent experiments indicated on the bars. Asterisks indicate significant differences from those calculated for cells expressing EGFP alone. Double asterisks correspond to $p < 0.001$, single asterisk shows $0.01 < p < 0.05$.

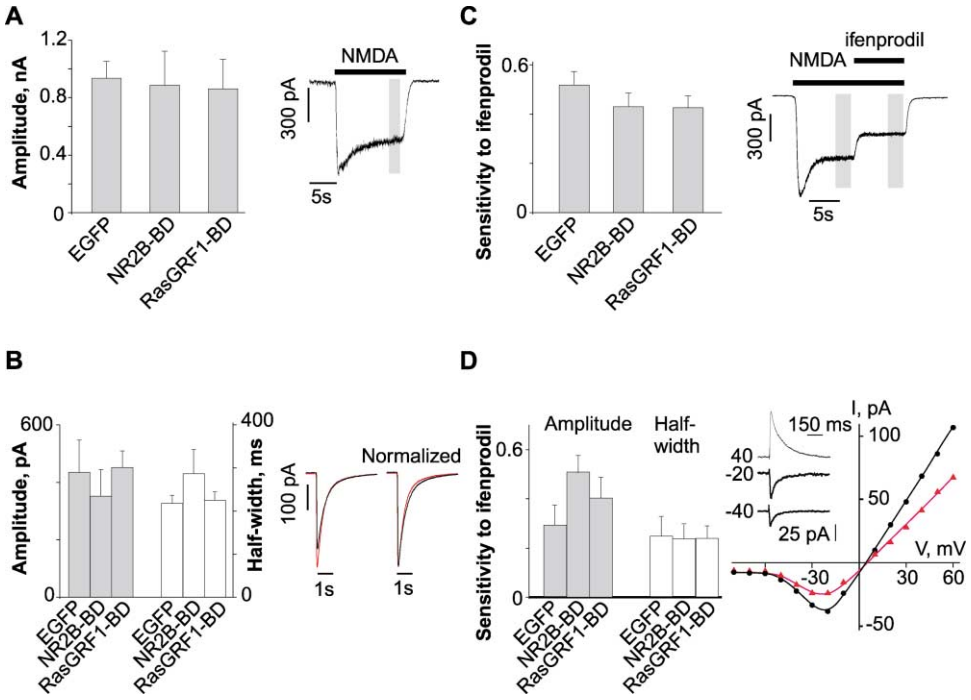

Figure 4. Expression of RasGRF1-BD or NR2B-BD Did Not Affect NMDA Receptor-Mediated Currents

(A) Average amplitudes (n = 10) of steady-state whole-cell currents evoked by bath application of 100 μM NMDA to neurons expressing GFP or GFP-BD. The trace illustrates the whole-cell current induced by bath application of 100 μM NMDA to a hippocampal neuron expressing GFP-RasGRF1-BD. Vertical bar indicates a segment of the recording used for calculation of mean value.

(B) Averaged spontaneous NMDA EPSCs in neurons expressing GFP or GFP-BD. Columns show the mean amplitude (filled) and half-width (open) of NMDA EPSCs obtained from five experiments. The traces are the averaged EPSCs (30 events) recorded from a neuron expressing GFP (black) or GFP-RasGRF1-BD (red).

(C) Ifenprodil sensitivity of whole-cell current induced by bath application of NMDA. The trace illustrating the recording procedure was obtained in a RasGRF1-BD-expressing neuron.

(D) Ifenprodil-sensitivity of the NMDA EPSPs evoked in CA3 pyramidal neurons in organotypic cultures of hippocampal slices. Columns represent the averaged (n = 7) ifenprodil sensitivity of the amplitude (filled) and half-width (open) of NMDAR EPSCs recorded at a holding potential of 40 mV. Ifenprodil sensitivity was defined as $(C_T - C_I)/C_T$ where C is the NMDAR-mediated current without (C_T) and with (C_I) 3 μM ifenprodil. The traces illustrate EPSCs recorded at different potentials from a neuron expressing RasGRF1-BD. The current-voltage relationships of the NMDA EPSCs were measured before (black circles) and during (red triangles) ifenprodil application.

main did not affect the average amplitude of the whole-cell current induced by bath application of NMDA (Figure 4A), or the mean amplitude and kinetics of the spontaneous NMDAR-mediated excitatory postsynaptic currents (NMDA EPSCs; Figure 4B).

The observation that RasGRF1 interacts with the NR2B, but not the NR2A or NR1 subunits, suggests that channels containing the NR2B subunits predominantly activate ERK. If this hypothesis is correct, then NR2B subunit-containing channel currents should be critical for ERK activation. Thus, it was important to determine whether expression of NR2B- and RasGRF1-blocking peptides modulated NR2B subunit-mediated current. To determine the NR2B-specific component of NMDA current, we employed ifenprodil, a noncompetitive antagonist of NR2B-containing NMDA receptors (Williams, 1993; Tovar and Westbrook, 1999). Figure 4C demonstrates that neither RasGRF1-BD nor NR2B-BD expression changed the proportion of ifenprodil-sensitive (NR2B) current stimulated by NMDA bath application to cultured neurons. It was not possible to estimate the proportion of the NR2B-mediated component in spontaneous NMDAR EPSCs in cultures of the dissociated neurons, since ifenprodil significantly reduced the frequency of the events. To circumvent this problem, we expressed NR2B-BD- or RasGRF-BD-blocking peptides in organotypic cultures of hippocampal slices and studied the effect of ifenprodil on the properties of the evoked NMDA EPSCs. Neither of the expressed peptides decreased the portion of the ifenprodil-sensitive component of the evoked EPSCs (Figure 4D). Confocal microscope-acquired images of cultured neurons transfected with either GFP-RasGRF1-BD or GFP-NR2B-BD and stained by NR2B antibody did not reveal any changes in the average number NR2B-positive clusters as compared to cells expressing GFP alone (Figure 5). Taken together, the data indicate that the blocking peptides specifically inhibited the NR2B-RasGRF1 interaction without affecting NR2B receptor number or NMDAR-dependent Ca^{2+} entry.

ERK Are Preferentially Activated via NR2B-Containing Channels

Given the specific coupling of RasGRF1 to NR2B subunit, we hypothesized that ERK is preferentially activated by Ca^{2+} entering neurons via NR2B-containing

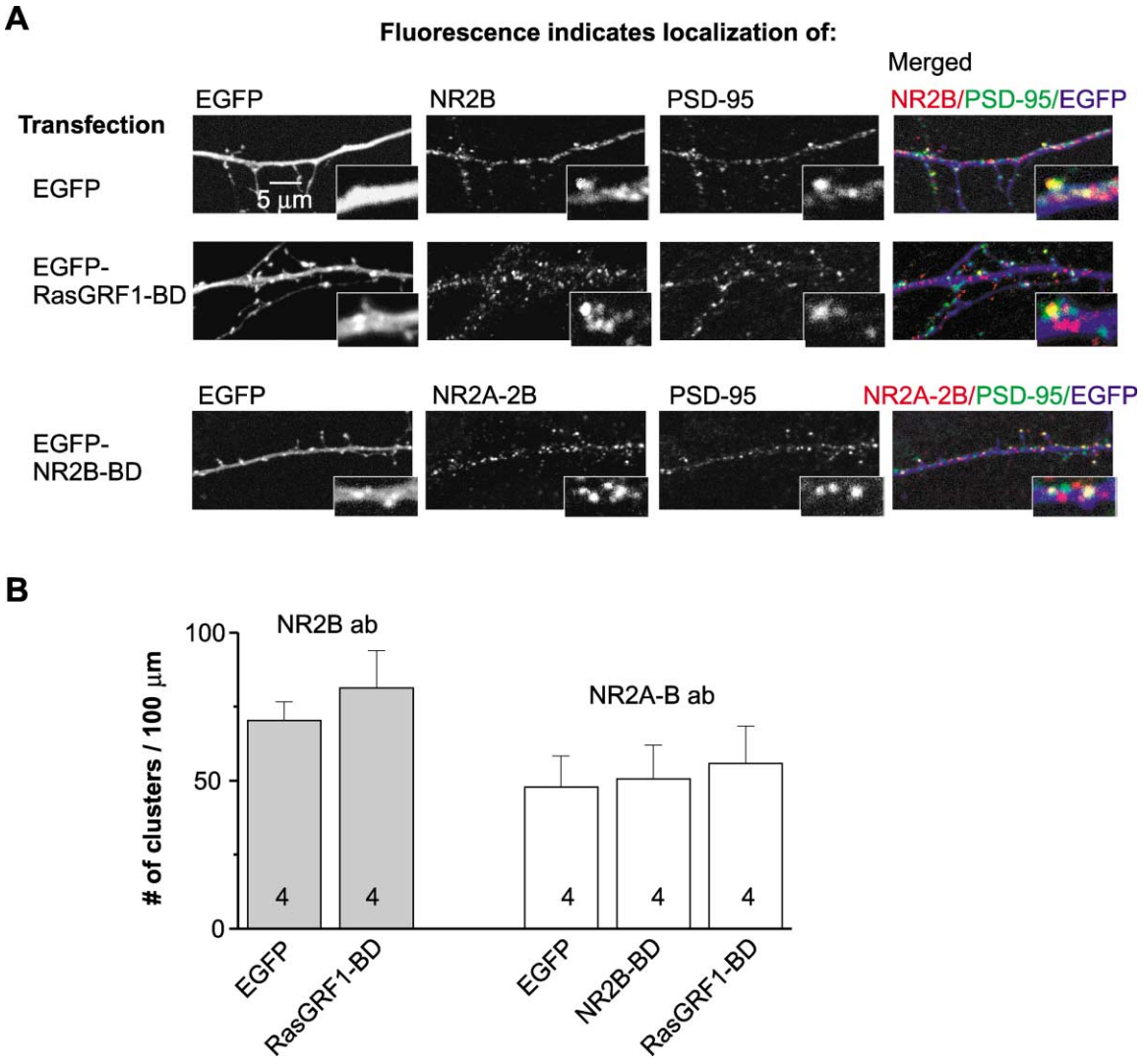

Figure 5. Blocking Peptides RasGRF1-BD and NR2B-BD Did Not Change the Localization or Density of NR2B or PSD-95

(A) Images of NR2B and PSD95 immunoreactive clusters.

(B) Averaged cluster density exhibited by NR2B antibody labeling (filled) or NR2A/B labeling (open).

NMDAR channels. The expression level of NR2B subunit in vivo remains stable during neuronal maturation, while NR2A expression progressively increases (Monyer et al., 1994; Sheng et al., 1994). In neurons cultured in vitro, the ratio between NR2B and NR2A subunits also decreases with age (Zhong et al., 1994; Li et al., 1998), and as a result there is an age-dependent decrease of the NMDA current sensitivity to the NR2B blocker, ifenprodil (Tovar and Westbrook, 1999; Hoffmann et al., 2000). In heterologous expression systems, ifenprodil at 3 μM inhibits up to 80% of NR2B-mediated current and has no effect on NR2A-mediated current (Williams, 1993; Tovar and Westbrook, 1999). In young neuronal cultures (neurons that presumably contain only NR2B/NR1 NMDA receptors [Zhong et al., 1994; Li et al., 1998]), ifenprodil inhibits ~70% of NMDA-mediated current and this inhibition decreased to 20%–30% in 3-week-old cultures (Tovar and Westbrook, 1999; Hoffmann et al., 2000). If ERK activation depended exclusively on NR2B-containing channels, then block of NR2B-specific current should significantly suppress NMDA-induced ERK activation independent of the proportion of NR2B-containing channels. In this case there should be no dependence of the proportion of ifenprodil-sensitive ERK activity on the proportion of ifenprodil-sensitive total NMDA current (see Experimental Procedures, Model). Alternatively, if ERK activation does not depend on whether its source was via an NR2A- or NR2B-containing channel, then the ifenprodil-sensitive portion of *ERK activity* will decrease in neurons expressing a lower fraction of NR2B subunit-containing channels. In agreement with previous studies (Tovar and Westbrook, 1999; Hoffmann et al., 2000), 3 μM ifenprodil suppressed 60% of NMDAR current in hippocampal neurons 8 div (Figures 6A and 6B). In the same cultures, we observed 70% inhibition of NMDAR-activated ERK (Figures 6A and 6B). The remaining 30% of the activity of ERK could be related to the uninhibited fraction of NR2B. During neuron maturation, the portion of the ifenprodil-sensitive NMDA current progressively decreased by ~25% with days in culture while the de-

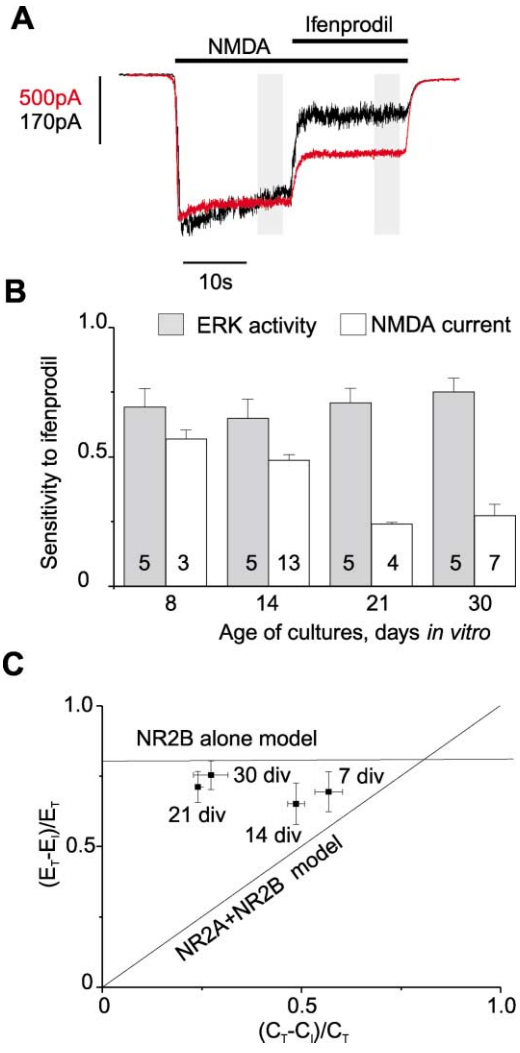

Figure 6. Ifenprodil Sensitivity of NMDA-Dependent ERK Activation and NMDA Receptor-Mediated Current in Hippocampal Neurons at Varying Days in Culture

(A) Ifenprodil-inhibited NR2B-containing current at 7 (black) and 21 (red) div (bath application of 100 μM NMDA). Vertical bars indicate segments of recordings used to calculate the mean values in (B).

(B) Ifenprodil-sensitive NMDA-induced current (open bars) decreased while the ifenprodil sensitivity of ERKs (filled bars) did not change with maturation. Ifenprodil sensitivity was defined as $(E_T - E_I)/E_T$ and $(C_T - C_I)/C_T$ where E and C are the NMDA-induced phospho-ERK immunoreactivity and ion current, respectively. Indices indicate measurements with (I) and without (T) 3 μM ifenprodil.

(C) Ifenprodil-sensitive ERK activity does not depend on the fraction of ifenprodil-sensitive NMDA current. Solid lines indicate the expected results in which ERK was activated by Ca^{2+} entering via all NMDA channels (NR2A+NR2B model) or by only NR2B-containing channels (NR2B-only model). Experimental data are taken from (B).

gree of ifenprodil-sensitive ERK activation did not change significantly (Figures 6A and 6B). This observation decidedly favors the model in which NR2B-containing channels are the dominant activators of the NMDA-dependent ERK pathway (Figure 6C).

Discussion

The ERK signaling cascade is crucial to neuronal cell survival (Grewal et al., 1999; Bonni et al., 1999) and neuronal plasticity, including different forms of LTP (Sweatt, 2001) and long-term memory (Adams and Sweatt, 2002). ERK activity in neurons is regulated by extracellular signals via multiple signaling pathways (Sweatt, 2001). NMDA receptor-stimulated activation ERK relies on Ca^{2+} influx via the NMDAR (Bading and Greenberg, 1991) and is critical for NMDAR-dependent forms of LTP (English and Sweatt, 1996; Adams and Sweatt, 2002). The mechanism of NMDAR coupling to ERK activation has not been determined, although PKA, PKC, CaMKII, and Ras have been proposed as putative intermediates in coupling NMDARs to ERKs (see Adams and Sweatt, 2002, for review).

Suppression of NMDA-dependent ERK activation by the dominant-negative form of RasGRF1 suggests that RasGRF1 is a crucial intermediate between the NMDAR and ERK activation. The interaction between NR2B and RasGRF1, and our demonstration that disruption of this interaction attenuated NMDA-dependent ERK activation, strongly suggests that the NR2B subunit directly links the NMDAR to ERK activation. This finding, together with fact that both ERK (Adams and Sweatt, 2002) and RasGRF1 (Giese et al., 2001) are important for hippocampal-dependent memory, suggests that the NMDAR-RasGRF1-ERK signaling chain is integral to hippocampal memory formation.

The physical association of RasGRF1 and NR2B makes RasGRF1 an ideal sensor for changes of $[Ca^{2+}]$ in the vicinity of the NMDA receptor and explains why NMDAR-initiated ERK activation is sensitive to spatially restricted Ca^{2+} elevation in proximity to the NMDAR (Hardingham et al., 2001). Such a local sensor allows separation of NMDAR inputs from other receptor signaling (e.g., BDNF, mGluRs, VDCC) that converge on the key regulatory element, ERK. The specific targeting of NR2B-RasGRF1 to ERK activation is highlighted by our finding that disruption of the NR2B-RasGRF1 complex resulted in abrogation of NMDAR-dependent ERK activation but did not affect NMDAR-dependent CREB phosphorylation on Ser133. Although both ERK and CREB activation depend on Ca^{2+} microdomains in the immediate vicinity of synaptic NMDA receptors (Hardingham et al., 2001), NMDAR-CREB signaling apparently does not involve RasGRF1.

Our data demonstrate that RasGRF1 specifically binds only the NR2B subunit of NMDAR. The experimental results favor a model in which NR2B-containing NMDA receptors serve as predominant activators of ERK. This finding is in agreement with numerous studies suggesting that the ERK-dependent processes, such as enhanced neuronal plasticity and the ability to learn and memorize, are related to expression of the NR2B subunits. In support of this hypothesis, previous investigators (Carmignoto and Vicini, 1992; Crair and Malenka, 1995) found that neurons from older animals (e.g., animals expressing lower proportion of NR2B [Monyer et al., 1994; Sheng et al., 1994]) displayed decreased neuronal plasticity. These authors suggested that changes in NMDAR properties underlie these differences. Furthermore, transgenic mice overexpressing the NR2B subunit in the forebrain were superior in learning and memory tests and exhibited facilitated synaptic potentiation (Tang et al., 1999). Disruption of the NR2B gene produced short-lived mice with impairment of major reflexes and abolished NMDA synaptic responses and

neuronal plasticity (Kutsuwada et al., 1996). Mice lacking the NR2A gene were viable with reduced but measurable spatial learning and neuronal plasticity (Sakimura et al., 1995; Kiyama et al., 1998). Since the NR2B subunit of the NMDAR, the subunit that is present mainly in juvenile neurons, interacts with RasGRF1, NR2B-RasGRF1-dependent signaling is likely to be involved in processes related to neuronal maturation and development.

In summary, we have found that physical coupling of RasGRF1 with the NR2B subunit of the NMDA receptor confines RasGRF1 to the vicinity of the NMDA channel, enabling it to sense Ca^{2+} microdomains around the channel mouth. We propose that NMDAR-dependent ERK activation is mediated by Ca^{2+}-dependent RasGRF1. The experiments described here emphasize the specific role of the NR2B subunit in targeting the ERK cascade.

Experimental Procedures

Yeast Two-Hybrid Screening

cDNAs encoding fragments of the rat NR2B C terminus were subcloned into the Gal4 binding domain fusion vector pGBKT7 (Clontech). These constructs were used for screening a rat brain library (Matchmaker pACT2, Clontech) expressed in AH109 yeast.

cDNA Constructs and Recombinant Proteins

NusA fusion proteins from rat NR2B (886–1310) and rat RasGRF1 (714–913) were subcloned into pET43.1 (Novagen) and expressed in BL21TrxLysS (Novagen) bacteria and 6His-NusA-fusion proteins affinity-purified on a cobalt-resin (Talon, Clontech).

For in vitro translation, fragments of rat NR2B and rat RasGRF1 were made by PCR with 5′-primers containing AU1- and HA-tag encoding sequences; amplified sequences were subcloned into pcDNA3.1. For 293T transfection, the following cDNAs were used: mouse RasGRF1 in pcDNA3 (gift of Dr. Zippel), GFP-rat NR2B, GFP-rat NR2A in pcDNA1.1 (gift of Dr. Vicini), and rat NR1 in pEGFP-C1 (Clontech). EGFP fusion constructs were made by subcloning cDNA fragments encoding different portions of NR2B and RasGRF1 into pEGFP-C1 (Clontech; details of all constructs provided on request). EGFP fusion constructs were transferred from pEGFP into pSinRep5 and used for preparation of the Sindbis pseudovirus gene transfer system according to the manufacturer's protocol (Invitrogen, Carlsbad, CA).

Cell Cultures and Transfections

HEK293T cells were grown in DMEM/F12 media supplemented with glycine, Na-hypoxanthine, penicillin/streptomycin, and 10% FBS. Cells were transfected using Lipofectamine 2000 (Invitrogen) and cultured for 48 hr.

Neurons from 18 day rat embryos were dissociated using trypsin and plated on coverslips coated with poly-L-lysine in minimal essential medium (MEM) with 10% NU serum (BD Biosciences, Le Pont de Claix, France) at densities of 30,000 cells/cm^2 as described (Brewer, 1995). On days 7 and 11 of culture incubation, half of the medium was changed to MEM with 2% B27 supplement (Invitrogen).

Cells were transfected with cDNA for EGFP fusion proteins (LipofectAMINE 2000; Invitrogen) or by pseudoviral infection using a Sindbis expression system (Invitrogen). Neurons were incubated with cDNA and LipofectAMINE for 2 hr, rinsed, and incubated with culture media (MEM with 2% of B27 supplement) 17 hr prior to the experiment. For viral delivery, neuronal cultures were incubated 30 min with pseudoviral constructs diluted 200–500× in culture media. Cultures were rinsed and incubated in media for 15 hr. 0.1% to 1.5% of neurons were fluorescent after expressing LipofectAMINE-delivered constructs while Sindbis infection yielded 1%–10% transfection efficiency. Most of the experiments were performed on 12–14 days in vitro (div) cultures unless otherwise indicated.

Organotypic cultures of hippocampal slices were prepared as described (Becq et al., 1999) according to modified technique of Stoppini et al. (1991). Hippocampal slices (400 μm) were cut from postnatal 7-day-old rat brains and incubated in culture medium in 5% CO_2. Infections were performed on the 6th day of slice incubation by local pressure injection of virus via a patch pipette (tip diameter ~1 μm) into the CA1 region of the hippocampus.

Immunoprecipitation and Pull-Down Assays

Mouse RasGRF1 in pcDNA3 (Martegani et al., 1992) was translated in vitro using the TNT system (Invitrogen) and [^{35}S]methionine. 5 μl of the translated RasGRF1 was incubated for 1 hr at 4°C with 2 μg of NusA-NR2B (886–1310) or NusA bound to Co^{2+} beads in 250 μl RIPA buffer (20 mM Tris-Cl [pH 8.0], 150 mM NaCl, 1% Triton X-100, 0.5% Na-Cholate, 0.1% SDS), washed with RIPA buffer, and solubilized in SDS sample buffer.

Transfected cells were solubilized in lysis buffer (100 mM Tris-Cl [pH 8.5], 500 mM NaCl, 1% Triton X-100) supplemented with complete protease inhibitor (Roche) and immunoprecipitated with NR2B (Santa Cruz, sc-9057), NR1, or NR2A (Chemicon) antibody (5 μg/ml), washed with lysis buffer, separated on SDS gel, and blotted on PVDF. Blots were probed with anti-RasGRF1 (Santa Cruz) and the appropriate NR subunit antibody. 6- to 8-week-old rat brain P2 microsomes were isolated and solubilized as described (Luo et al., 1997). 80 μg of solubilized protein were immunoprecipitated with NR2B, RasGRF1, or pooled rabbit IgG, and immunoprecipitated proteins were probed on Western blot with RasGRF1 and NR2B antibodies. All immunoprecipitation experiments were only taken as valid if repeated 3–5 times with similar results. Routine negative controls with antigen pre-absorption were carried out for antibodies used in immunoprecipitation experiments. Also, all immunoprecipitating antibodies were tested for the cross-reactivity with in vitro translated co-immunoprecipitated molecules. Both tests proved their specificity and the absence of cross-reactivity of the immunoprecipitating antibody.

For in vitro binding experiments, equimolar amounts of in vitro translated ^{35}S-labeled proteins (calculated from radioactivity of the excised protein band and cysteine content in the specific fragment) were incubated with a 3-fold molar excess of translated RasGRF1 for 30 min at 30°C, diluted with RIPA buffer, and immunoprecipitated with anti-HA-agarose (Santa Cruz). In competition experiments, RasGRF1 and NR2B were immunoprecipitated for 2 hr at 4°C from solubilized rat brain microsomes in the presence of 10 μM NusA, 10 μM NusA-RasGRF1-BD, or 5 μM NusA-NR2B-BD.

Immunocytochemistry and Confocal Microscopy of Cultured Hippocampal Neurons

Phospho-ERK Immunocytochemistry

Three hours before stimulation, TTX (1 μM), CNQX (40 μM), APV (100 μM), and nimodipine (5 μM) were added to neurons. For stimulation, coverslips with neurons were transferred into the following solutions.

(1) 100 μM NMDA, 10 μM glycine, 1 μM TTX, 40 μM CNQX, 5 μM nimodipine dissolved in culture media and incubated for 3 min. Under these conditions, longer (10 min) stimulation with NMDA resulted in significantly lower ERK stimulation.

(2) 10 μM bicuculline, 10 μM glycine, 5 μM nimodipine (without TTX, APV, or CNQX) in culture media incubated for 5 min.

(3) 50 mM KCl included in modified extracellular media: 120 mM NaCl, 10 mM HEPES, 10 mM D-glucose, 2.0 mM $CaCl_2$, 2.0 mM $MgCl_2$, 1 μM TTX, 40 μM CNQX, 100 μM APV and incubated for 10 min.

(4) 100 ng/ml BDNF in culture media with TTX (1 μM), CNQX (40 μM), APV (100 μM), and nimodipine (5 μM), incubated for 10 min.

After stimulation, neurons were fixed with 4% formaldehyde and labeled with rabbit anti-phospho-p44/42 ERK antibody (Cell Signaling) and with mouse anti-MAP2 antibody (Sternberger Monoclonals). Cy3-conjugated goat anti-rabbit IgG and Cy5-conjugated goat anti-mouse IgG (Jackson ImmunoResearch Laboratories, West Grove, PA) were secondary antibodies. NMDA and all antagonists were from Tocris Neuramin. BDNF was from Calbiochem.

Images were acquired with an Olympus Fluoview-500 confocal microscope (40×; 1.0 NA) and quantified using Olympus Fluoview software. In each experiment, the pERK fluorescence of the cell soma was measured for 25 neurons taken from consecutive fields. Phospho-ERK fluorescence data were normalized to the values obtained in nontransfected cells after NMDA stimulation. The back-

ground fluorescence (mean fluorescence of nonstimulated neurons) was subtracted prior to normalization.

Immunocytochemistry of NR2B Subunits

Coverslips with cultured neurons were fixed with 4% paraformaldehyde, permeabilized with 0.3% Triton X-100, and blocked in 10% goat serum in PBS. A rabbit polyclonal antibody against the N terminus of the NR2B subunit of the NMDA receptor (AB1557P, Chemicon, Temecula, CA) was used for detection in neurons expressing GFP and RasGRF1-BD. These antibodies could not be used for study of the NR2B subunit distribution in neurons expressing NR2B-BD since they recognized the expressed construct. The distribution of NR2A/B subunit was determined using polyclonal antibody AB1548 (Chemicon). A mouse monoclonal antibody (clone K 28/43, Upstate, Waltham, MA) was used to detect PSD-95. Secondary antibodies were the same as that used for detection of ERK and MAP2. To quantify the distribution of clusters in transfected cells, we first focused on dendrites of neurons expressing the EGFP-fluorescent construct. Thereafter, fluorescent images of GFP, NR2B, and PSD-95 were acquired confocally (60×; NA 1.4 objective, zoom 5). Cluster density and brightness were analyzed with the MetaMorph Imaging System (Universal Imaging, Westchester, PA). Ten neurons were analyzed from each experiment (3–4 dendritic regions for each neuron).

Electrophysiological Recordings

Electrophysiological recordings from neurons were performed 19–24 hr after transfection or 14–20 hr after viral infection. No difference between transfected and infected neurons was observed. Neurons were continuously perfused with extracellular solution containing (in mM): 140 NaCl, 2.5 KCl, 20 HEPES, 20 D-glucose, 2.0 $CaCl_2$, 0.02 glycine, 0.01 bicuculline, 0.01 CNQX, and 0.001 tetrodotoxin (TTX) with no added Mg^{2+} (pH 7.4). Measurements of the spontaneous NMDA-EPSCs were recorded in the absence of TTX. NMDA (100 μM) or NMDA and ifenprodil (3 μM) were dissolved in the bath solution and delivered by gravity via a double-barrel pipe displaced 70–100 μm from the neuron. Recording electrodes (2–4 MΩ) were pulled from borosilicate glass (TW150F-15; World Precision Instruments), filled with solution containing (in mM) 115 Cs methanesulfonate, 20 CsCl, 10 HEPES, 2.5 $MgCl_2$, 4 Na_2-ATP (adenosine triphosphate), 0.4 Na-GTP (guanosine triphosphate), 10 mM Na-phosphocreatine, and 0.6 mM EGTA (pH 7.2). Ifenprodil was from RBI.

Recordings were made using an Axopatch-200A amplifier and pCLAMP acquisition software (Axon Instruments). Series resistance varied from 6 to 8 MΩ and electronic compensation for series resistance was employed. Data were low-pass filtered at 2 kHz and acquired at 10 kHz. NMDA receptor-mediated EPSCs were analyses using Mini Analysis software (Synaptosoft, Decatur, GA). The same number of events was compared in each set of experiments.

Organotypic Hippocampal Cultures

For electrophysiological recordings, slices were placed in a recording chamber and perfused with ACSF including in mM: 119 NaCl, 2.5 KCl, 2 $CaCl_2$, 2 $MgCl_2$, 26 $NaHCO_3$, 1 NaH_2PO_4, 11 glucose, 0.01 bicuculline, 0.01 CNQX, 0.002 2-chloroadenosine (pH 7.4), in 5% CO_2/95% O_2. Synaptic responses were evoked by bipolar electrode with monophasic voltage pulses (1–10 V, 200 μs). The stimulating electrodes were placed over Schaeffer collateral fibers. NMDA-evoked EPSCs were recorded at different holding potentials before, during, and after ifenprodil application in order to measure the I-V relationship. For analysis, at least 5 NMDA-evoked EPSCs were averaged for every experimental condition.

Statistical Analysis

All population data were expressed as mean ± SEM. The Student's t test was employed to examine the statistical significance of the differences between groups of data.

Model

If C_T is total NMDA-activated current, C_I is the current elicited in the presence ifenprodil, α is the coefficient of residual activity of NR2B channels in the presence of ifenprodil, and A and B are the number of NR2A- and NR2B-containing NMDA channels, then $C_T = n(A + B)$, $C_I = n(A + \alpha B)$ and the portion of the current via NR2B-containing receptor is $B/(A + B) = (C_T - C_I)/(1 - \alpha C_T)$.

We define E_T and E_I as the total and ifenprodil-insensitive ERK activity, respectively. For a model in which Ca^{2+} entering neurons via both NR2A- and NR2B-containing channels (A + B model), $E_T = k(A + B)$ and $E_I = k(A + \alpha B)$. The degree of ERK activity inhibited by ifenprodil will be: $(E_T - E_I)/E_T = (1 - \alpha)B/(A + B) = (C_T - C_I)/C_T$. In other words, normalized ifenprodil-sensitive ERK activity will be directly proportional to the normalized ifenprodil-sensitive NMDA current. For a model in which the Ca^{2+} enters neurons only via NR2B-containing channels (B-only model), $E_T = kB$ and $E_I = k\alpha B$. The normalized ERK activity inhibited by ifenprodil will be: $(E_T - E_I)/E_T = (1 - \alpha)$ and will not correlate with ifenprodil-sensitive NMDA current.

Acknowledgments

We are grateful to Renata Zippel for RasGRF1 cDNA, Stefano Vicini for GFP-NR2A and GFP-NR2B constructs, and Helène Becq for preparing organotypic cultures of hippocampal slices. This work was supported by Howard Hughes Medical Institute (D.E.C.), INSERM (I.M.), and the Foundation for Medical Research (G.K. and Y.B.-A.).

Received: June 10, 2003
Revised: August 20, 2003
Accepted: September 19, 2003
Published: November 12, 2003

References

Abel, T., and Lattal, K.M. (2001). Molecular mechanisms of memory acquisition, consolidation and retrieval. Curr. Opin. Neurobiol. *11*, 180–187.

Adams, J.P., and Sweatt, J.D. (2002). Molecular psychology: roles for the ERK MAP kinase cascade in memory. Annu. Rev. Pharmacol. Toxicol. *42*, 135–163.

Bading, H., and Greenberg, M.E. (1991). Stimulation of protein tyrosine phosphorylation by NMDA receptor activation. Science *253*, 912–914.

Bayer, K.U., De Koninck, P., Leonard, A.S., Hell, J.W., and Schulman, H. (2001). Interaction with the NMDA receptor locks CaMKII in an active conformation. Nature *411*, 801–805.

Becq, H., Bosler, O., Geffard, M., Enjalbert, A., and Herman, J.P. (1999). Anatomical and functional reconstruction of the nigrostriatal system in vitro: selective innervation of the striatum by dopaminergic neurons. J. Neurosci. Res. *58*, 553–566.

Bonni, A., Brunet, A., West, A.E., Datta, S.R., Takasu, M.A., and Greenberg, M.E. (1999). Cell survival promoted by the Ras-MAPK signaling pathway by transcription-dependent and -independent mechanisms. Science *286*, 1358–1362.

Brambilla, R., Gnesutta, N., Minichiello, L., White, G., Roylance, A.J., Herron, C.E., Ramsey, M., Wolfer, D.P., Cestari, V., Rossi-Arnaud, C., et al. (1997). A role for the Ras signalling pathway in synaptic transmission and long-term memory. Nature *390*, 281–286.

Brewer, G.J. (1995). Serum-free B27/neurobasal medium supports differentiated growth of neurons from the striatum, substantia nigra, septum, cerebral cortex, cerebellum, and dentate gyrus. J. Neurosci. Res. *42*, 674–683.

Carmignoto, G., and Vicini, S. (1992). Activity-dependent decrease in NMDA receptor responses during development of the visual cortex. Science *258*, 1007–1011.

Chen, H.J., Rojas-Soto, M., Oguni, A., and Kennedy, M.B. (1998). A synaptic Ras-GTPase activating protein (p135 SynGAP) inhibited by CaM kinase II. Neuron *20*, 895–904.

Crair, M.C., and Malenka, R.C. (1995). A critical period for long-term potentiation at thalamocortical synapses. Nature *375*, 325–328.

Cull-Candy, S., Brickley, S., and Farrant, M. (2001). NMDA receptor subunits: diversity, development and disease. Curr. Opin. Neurobiol. *11*, 327–335.

Dolmetsch, R.E., Pajvani, U., Fife, K., Spotts, J.M., and Greenberg,

M.E. (2001). Signaling to the nucleus by an L-type calcium channel-calmodulin complex through the MAP kinase pathway. Science *294*, 333–339.

English, J.D., and Sweatt, J.D. (1996). Activation of p42 mitogen-activated protein kinase in hippocampal long term potentiation. J. Biol. Chem. *271*, 24329–24332.

Farnsworth, C.L., Freshney, N.W., Rosen, L.B., Ghosh, A., Greenberg, M.E., and Feig, L.A. (1995). Calcium activation of Ras mediated by neuronal exchange factor Ras-GRF. Nature *376*, 524–527.

Ghosh, A., and Greenberg, M.E. (1995). Calcium signaling in neurons: molecular mechanisms and cellular consequences. Science *268*, 239–247.

Giese, K.P., Friedman, E., Telliez, J.B., Fedorov, N.B., Wines, M., Feig, L.A., and Silva, A.J. (2001). Hippocampus-dependent learning and memory is impaired in mice lacking the Ras-guanine-nucleotide releasing factor 1 (Ras-GRF1). Neuropharmacology *41*, 791–800.

Ginty, D.D., Kornhauser, J.M., Thompson, M.A., Bading, H., Mayo, K.E., Takahashi, J.S., and Greenberg, M.E. (1993). Regulation of CREB phosphorylation in the suprachiasmatic nucleus by light and a circadian clock. Science *260*, 238–241.

Grewal, S.S., York, R.D., and Stork, P.J. (1999). Extracellular-signal-regulated kinase signalling in neurons. Curr. Opin. Neurobiol. *9*, 544–553.

Hardingham, G.E., Arnold, F.J., and Bading, H. (2001). A calcium microdomain near NMDA receptors: on switch for ERK-dependent synapse-to-nucleus communication. Nat. Neurosci. *4*, 565–566.

Hoffmann, H., Gremme, T., Hatt, H., and Gottmann, K. (2000). Synaptic activity-dependent developmental regulation of NMDA receptor subunit expression in cultured neocortical neurons. J. Neurochem. *75*, 1590–1599.

Iida, N., Namikawa, K., Kiyama, H., Ueno, H., Nakamura, S., and Hattori, S. (2001). Requirement of Ras for the activation of mitogen-activated protein kinase by calcium influx, cAMP, and neurotrophin in hippocampal neurons. J. Neurosci. *21*, 6459–6466.

Impey, S., Obrietan, K., and Storm, D.R. (1999). Making new connections: role of ERK/MAP kinase signaling in neuronal plasticity. Neuron *23*, 11–14.

Kim, J.H., Liao, D., Lau, L.F., and Huganir, R.L. (1998). SynGAP: a synaptic RasGAP that associates with the PSD-95/SAP90 protein family. Neuron *20*, 683–691.

Kiyama, Y., Manabe, T., Sakimura, K., Kawakami, F., Mori, H., and Mishina, M. (1998). Increased thresholds for long-term potentiation and contextual learning in mice lacking the NMDA-type glutamate receptor epsilon1 subunit. J. Neurosci. *18*, 6704–6712.

Kurino, M., Fukunaga, K., Ushio, Y., and Miyamoto, E. (1995). Activation of mitogen-activated protein kinase in cultured rat hippocampal neurons by stimulation of glutamate receptors. J. Neurochem. *65*, 1282–1289.

Kutsuwada, T., Sakimura, K., Manabe, T., Takayama, C., Katakura, N., Kushiya, E., Natsume, R., Watanabe, M., Inoue, Y., Yagi, T., et al. (1996). Impairment of suckling response, trigeminal neuronal pattern formation, and hippocampal LTD in NMDA receptor epsilon 2 subunit mutant mice. Neuron *16*, 333–344.

Li, J.H., Wang, Y.H., Wolfe, B.B., Krueger, K.E., Corsi, L., Stocca, G., and Vicini, S. (1998). Developmental changes in localization of NMDA receptor subunits in primary cultures of cortical neurons. Eur. J. Neurosci. *10*, 1704–1715.

Luo, J., Wang, Y., Yasuda, R.P., Dunah, A.W., and Wolfe, B.B. (1997). The majority of N-methyl-D-aspartate receptor complexes in adult rat cerebral cortex contain at least three different subunits (NR1/NR2A/NR2B). Mol. Pharmacol. *51*, 79–86.

Martegani, E., Vanoni, M., Zippel, R., Coccetti, P., Brambilla, R., Ferrari, C., Sturani, E., and Alberghina, L. (1992). Cloning by functional complementation of a mouse cDNA encoding a homologue of CDC25, a *Saccharomyces cerevisiae* RAS activator. EMBO J. *11*, 2151–2157.

Monyer, H., Burnashev, N., Laurie, D.J., Sakmann, B., and Seeburg, P.H. (1994). Developmental and regional expression in the rat brain and functional properties of four NMDA receptors. Neuron *12*, 529–540.

Oh, J.S., Chen, H.-J., Rojas-Soto, M., Oguni, A., and Kennedy, M.B. (2002). Erratum. Neuron *33*, 151.

Payne, D.M., Rossomando, A.J., Martino, P., Erickson, A.K., Her, J.H., Shabanowitz, J., Hunt, D.F., Weber, M.J., and Sturgill, T.W. (1991). Identification of the regulatory phosphorylation sites in pp42/mitogen-activated protein kinase (MAP kinase). EMBO J. *10*, 885–892.

Platenik, J., Kuramoto, N., and Yoneda, Y. (2000). Molecular mechanisms associated with long-term consolidation of the NMDA signals. Life Sci. *67*, 335–364.

Sakimura, K., Kutsuwada, T., Ito, I., Manabe, T., Takayama, C., Kushiya, E., Yagi, T., Aizawa, S., Inoue, Y., and Sugiyama, H. (1995). Reduced hippocampal LTP and spatial learning in mice lacking NMDA receptor epsilon 1 subunit. Nature *373*, 151–155.

Sheng, M., Cummings, J., Roldan, L.A., Jan, Y.N., and Jan, L.Y. (1994). Changing subunit composition of heteromeric NMDA receptors during development of rat cortex. Nature *368*, 144–147.

Shou, C., Farnsworth, C.L., Neel, B.G., and Feig, L.A. (1992). Molecular cloning of cDNAs encoding a guanine-nucleotide-releasing factor for Ras p21. Nature *358*, 351–354.

Stoppini, L., Buchs, P.A., and Muller, D. (1991). A simple method for organotypic cultures of nervous tissue. J. Neurosci. Methods *37*, 173–182.

Sturani, E., Abbondio, A., Branduardi, P., Ferrari, C., Zippel, R., Martegani, E., Vanoni, M., and Denis-Donini, S. (1997). The Ras guanine nucleotide exchange factor CDC25Mm is present at the synaptic junction. Exp. Cell Res. *235*, 117–123.

Sweatt, J.D. (2001). The neuronal MAP kinase cascade: a biochemical signal integration system subserving synaptic plasticity and memory. J. Neurochem. *76*, 1–10.

Tang, Y.P., Shimizu, E., Dube, G.R., Rampon, C., Kerchner, G.A., Zhuo, M., Liu, G., and Tsien, J.Z. (1999). Genetic enhancement of learning and memory in mice. Nature *401*, 63–69.

Tovar, K.R., and Westbrook, G.L. (1999). The incorporation of NMDA receptors with a distinct subunit composition at nascent hippocampal synapses in vitro. J. Neurosci. *19*, 4180–4188.

Tonini, R., Franceschetti, S., Parolaro, D., Sala, M., Mancinelli, E., Tininini, S., Brusetti, R., Sancini, G., Brambilla, R., Martegani, E., et al. (2001). Involvement of CDC25Mm/Ras-GRF1-dependent signaling in the control of neuronal excitability. Mol. Cell. Neurosci. *18*, 691–701.

Vanoni, M., Bertini, R., Sacco, E., Fontanella, L., Rieppi, M., Colombo, S., Martegani, E., Carrera, V., Moroni, A., Bizzarri, C., et al. (1999). Characterization and properties of dominant-negative mutants of the ras-specific guanine nucleotide exchange factor CDC25(Mm). J. Biol. Chem. *274*, 36656–36662.

West, A.E., Chen, W.G., Dalva, M.B., Dolmetsch, R.E., Kornhauser, J.M., Shaywitz, A.J., Takasu, M.A., Tao, X., and Greenberg, M.E. (2001). Calcium regulation of neuronal gene expression. Proc. Natl. Acad. Sci. USA *98*, 11024–11031.

Williams, K. (1993). Ifenprodil discriminates subtypes of the N-methyl-D-aspartate receptor: selectivity and mechanisms at recombinant heteromeric receptors. Mol. Pharmacol. *44*, 851–859.

Xia, Z., Dudek, H., Miranti, C.K., and Greenberg, M.E. (1996). Calcium influx via the NMDA receptor induces immediate early gene transcription by a MAP kinase/ERK-dependent mechanism. J. Neurosci. *16*, 5425–5436.

Zhong, J., Russell, S.L., Pritchett, D.B., Molinoff, P.B., and Williams, K. (1994). Expression of mRNAs encoding subunits of the N-methyl-D-aspartate receptor in cultured cortical neurons. Mol. Pharmacol. *45*, 846–853.

Zhu, J.J., Qin, Y., Zhao, M., Van Aelst, L., and Malinow, R. (2002). Ras and Rap control AMPA receptor trafficking during synaptic plasticity. Cell *110*, 443–455.

Zippel, R., Gnesutta, N., Matus-Leibovitch, N., Mancinelli, E., Saya, D., Vogel, Z., Sturani, E., Renata, Z., Nerina, G., Noa, M.L., et al. (1997). Ras-GRF, the activator of Ras, is expressed preferentially in mature neurons of the central nervous system. Brain Res. Mol. Brain Res. *48*, 140–144.